JOURNAL OF CATALYSIS **169,** 503–509 (1997)
ARTICLE NO. CA971731

$NiPS_3$ Intercalates as Catalysts for the Oxidation of Sulfide Ions: Synthesis, Catalytic Activity, and XPS Study

Elina Manova,*,† Claude Severac,‡ Atanas Andreev,* and René Clément†

*Institute of Catalysis, Bulgarian Academy of Sciences, Acad. G. Bontchev Str., bl. 11, 1113 Sofia, Bulgaria; and †Laboratoire de Chimie Inorganique, URA 420, Bat 420, and ‡Laboratoire de Métallurgie Structurale, URA 1107, Bat 410, University of Paris XI, 91405 Orsay Cedex, France

Received January 14, 1997; revised March 24, 1997; accepted March 24, 1997

Several intercalates of layered $NiPS_3$ have been synthesized by reaction of this compound with aqueous solutions of sodium sulfide and subsequent cation exchange or polymer insertion. The catalytic efficiency of these intercalates for the oxydation of sulfide ions into elemental sulfur by dioxygen has been studied. Results show that these intercalates have a greater efficiency than pristine $NiPS_3$ (higher reaction rate, smaller activation energy, suppression of any induction period). The electronic structure of the intercalates has been studied mainly by XPS of the Ni, P, and S atoms. Although the chemistry accompanying the intercalation processes appears complex (small losses of phosphorus, appearance of phosphate, and thiophosphate PS_4^{3-} species), the catalytic efficiency of the intercalates is correlated to their ability to be reduced in depth when brought in contact with aqueous sodium sulfide. Our results are consistent with a previously suggested catalytic mechanism based on sequences of intercalation/deintercalation processes of sodium ions associated to redox modifications of the host lattice.

INTRODUCTION

Sulfide ions are one of the most powerful pollutants in industrial waste water and sewage water. Their oxidation by oxygen from the air

$$S^{2-} + \frac{1}{2}O_2 + H_2O \rightarrow S^0 + 2OH^- \qquad [1]$$

leads to the formation of nonpoisonous elemental sulfur which is further removed by filtration or biological treatment. This process is of great importance for environmental protection and determines the necessity of design of novel effective industrial catalysts (1).

Previous studies (2) have shown that $NiPS_3$ catalyzes reaction [1]. $NiPS_3$ is a member of a class of layered compounds with general formula MPS_3, where M is a bivalent transition metal (for a review, see Refs. 3, 4). These thiophosphates manifest a unique ability to form intercalates by means of either charge transfer or cation exchange (5). In contrast to other members of the family, $NiPS_3$ does not form intercalates by cation exchange, probably because of the greater covalent character of the Ni–S bonds. Numerous studies dealing with lithium insertion—either chemically or electrochemically—have shown that $NiPS_3$ possesses a redox intercalation chemistry based on electron transfer from lithium to the host material (6–11).

An attempt has been made to explain the catalytic activity of $NiPS_3$ in the reaction of sulfide ion oxidation on the basis of a mechanism involving sequences of intercalation/deintercalation processes of sodium ions (2). Actually our group had previously shown that $NiPS_3$ was able to react with sodium sulfide aqueous solutions to give a sodium intercalate (12). However the insertion mechanism was not clear, as a significant loss of P(IV) atoms was observed.

The goal of this paper is twofold: (i) examine whether $NiPS_3$ intercalates are more efficient catalysts as pure $NiPS_3$; (ii) obtain a better understanding of the electronic structure of the $NiPS_3$ intercalates and of the redox processes that take place along the catalytic process. For this purpose, several $NiPS_3$ intercalates have been synthesized and characterized by XPS and their catalytic efficiency for reaction [1] has been studied.

METHODS

1. Synthesis and Characterization of Intercalates

Pure $NiPS_3$ was prepared by heating a stoichiometric mixture of the elements (99% purity) in a sealed evacuated quartz tube, following a procedure described elsewhere (13).

A sodium intercalate $Na_x(H_2O)_yNiPS_3$ **1** was synthesized by reaction of 0.5 M Na_2S aqueous solution (20 ml) over $NiPS_3$ (100 mg) in an argon atmosphere for 24 h. The powder was then washed several times with a degassed 0.1 M aqueous solution of NaCl and dried under argon. Washing with pure water was observed to cause partial dispersion of **1**.

Pyridinium (pyH) and tetraethylammonium (Et_4N) intercalates of $NiPS_3$ (resp. **2** and **3**) were obtained by treating the sodium intercalate **1** with an ethanolic solution (10 ml) of Et_4NCl (1 g) or pyHCl (3 g), respectively, for 12 h at

0021-9517/97 $25.00

room temperature under argon. The products were washed several times with ethanol and dried in air.

Following a procedure already employed for $MnPS_3$ intercalates (14), polyethylene glycol (PEG, M.W. 6000) was also inserted in **1** by treating **1** with a 1 : 1 methanol : water solution (15 ml) of PEG (1 g) at 60°C for 4 h (intercalate **4**).

To simulate catalytic conditions, see below, intercalates **2**, **3**, and **4** themselves were retreated by an Na_2S aqueous solution. Under these conditions, the pyridinium intercalate **2** gave a compound noted **5**, but intercalates **3** and **4** dispersed too much and the resulting solids could not be isolated.

Elemental analysis data were obtained from the CNRS analytical service. The C, H, and N content was measured by gas chromatography after combustion of the samples. The content of the other elements was determined after mineralization (coulometry for S, colorimetry on the phosphomolybdic compound for P, atomic absorption spectroscopy for the metals). X-ray powder diffraction patterns were acquired by means of Siemens diffractometer fitted with a copper anticathode. Infrared spectra in the range 4000–200 cm^{-1} were obtained as KBr pellets using Perkin–Elmer 883 Spectrometer, but the range below 300 cm^{-1} was obscured by the absorption of the KBr matrix. The possibility of exchange of Na^+ ions for K^+ ions during the preparation of the pellets, as well as the possible insertion of Br^- ions have not been considered.

2. *XPS Measurements*

XPS measurements were made by using a Leybold LHS 10 spectrometer equipped with a standart Mg/Al $K\alpha$ X-ray source and a 180° concentric hemispherical analyser (CHA). The Al $K\alpha$ X-ray line (1486.6 eV) was used for photoelectron excitation. The spectrometer was calibrated by using the photoemission lines of Au (Au $4f_{7/2}$, 84 eV) and Cu (Cu $2p_{3/2}$, 932.7 eV).

The powder samples were pressed onto sample holders and introduced in the spectrometer chamber having a pressure of 1×10^{-9} Torr. The cleanliness of the surface was checked through the absence or weakness of oxygen 1*s* XPS signal. In order to compensate for the charging of insulating samples during the photoelectron ejecting process, all the spectra were referenced to the photoelectron line of Au ($4f_{7/2}$), $E_b = 84.5$ eV, by vacuum deposition of gold onto the samples. Such charging corrections ranged from -0.3 to -2.2 eV. The region of interest was scanned before and after gold deposition to make sure that no extraneous peaks had originated by this method of standardization. The total resolution is about 1 eV and experimental errors in binding energies are ± 0.1 eV.

The XPS signals were analyzed by using a peak synthesis program in which the fitting peaks of the experimental curve are defined thanks to a combination of gaussian and lorenzian distributions ($L/G < 20\%$). For the analysis the full width at half maximum (FWHM), the peak center and the relative peak intensities of the observed spectra were determined.

3. *Catalytic Activity*

The catalytic activity of the samples (typically 0.01 g) for sulfide ion oxidation was measured under static conditions through the amount of oxygen consumed by an aqueous solution of Na_2S (20 ml). The measurements were carried out at different temperatures and concentrations of the S^{2-} ions. The catalytic activity is expressed as moles of S^{2-} ions oxidized per gram atom of Ni (mol S^{2-}/g · at Ni).

4. *Electrochemical Measurements*

An electrode containing $NiPS_3$ (or the various intercalates) was prepared by pressing the powdered sample in a platinum holder, whose external surface was isolated from the solution by a glass coating, as in Ref. (2). The potential difference between this electrode and a calomel electrode was measured. Measurements were carried out in a glass cell, in which an aqueous Na_2S solution (2 g/liter) was introduced. The cell allows the system to be blown through with argon and oxygen, alternatively.

RESULTS

All intercalates were characterized by powder X-ray diffraction. Powder of the intercalates was spread on the sample holder. Because of the platelet morphology of the crystals, this procedure leads to an enhancement of the intensity of the 00l reflections. The spectra show sharp 00l diffraction peaks indicating an increase of the interlayer distance. Complete intercalation was ascertained by disappearance of the 00l reflections of pure $NiPS_3$. Table 1 presents interlayer distances of the investigated intercalates (0.645 nm for pristine $NiPS_3$), elemental analysis data, and calculated formula. As already noted in Ref. (12), a systematic and significant loss of phosphorus with respect to sulfur and nickel is observed. The water content of the compounds is estimated from the hydrogen content.

The infrared spectra of the intercalates show bands which can be attributed to the host lattice and to the guest species (Figs. 1a–1d). Bands due to internal modes of the intercalated species were observed in the range 4000–700 cm^{-1}, whereas vibrations characteristic of the host lattice are present below 700 cm^{-1}. The $\nu(PS_3)$ stretching mode appears as a single strong band at 570 cm^{-1} in pure $NiPS_3$. This band is usually split in two components at 605 and 555 cm^{-1} in all intercalates obtained by ion exchange (5). The IR pattern in the $NiPS_3$ intercalates in this range appear different and more complex. The sodium intercalate **1** and the tetraethylammonium **3** (not shown) exhibit two bands at 570 and 515 cm^{-1}. The pyridinium intercalate **2**

TABLE 1

Elemental Analysis Data and Calculated Interlayer Spacings of the $NiPS_3$ Intercalates

Proposed formula	% Ni	% P	% S	% Na	% H	% C	% N	Spacing (nm)
$Na_{0.64}NiP_{0.9}S_3(H_2O)_{1.2}$ **1**	26.35	12.35	42.45	6.50	1.05			1.245
$Na_{0.19}NiP_{0.82}S_3(H_2O)_{0.6}(C_8H_{20}N)_{0.13}$ **3**	27.51	11.90	45.08	2.05	1.65	6.30	0.80	1.133
$Na_{0.3}NiP_{0.9}S_3(H_2O)_{1.8}(CH_2{-}CH_2O)_{1.0}$ **4**	18.86	7.94	27.69	2.04	2.33	7.39		1.498
$Ni_{0.92}P_{0.8}S_3(C_5H_6N)_{0.2}$ **2**	25.77	11.85	45.90	620 ppm	5.56	0.71	1.02	0.977
$Na_{0.59}NiP_{0.92}S_3(H_2O)_{0.45}(C_5H_6N)_{0.01}$ **5**	26.08	12.50	41.95	5.87	0.47	0.83	0.30	1.240

still shows the 575 cm^{-1} band but this band is asymetric and a broad shoulder is present between 540 and 500 cm^{-1}. In addition, a sharp band is present at 615 cm^{-1}. When **2** is further retreated by Na_2S to give **4**, the IR pattern in the P–S region appears intermediate between those of **1** and **2**, i.e., persistence of the 570 cm^{-1} strong band, decrease of the intensity of the 615 cm^{-1}, and appearance of a small band at 520 cm^{-1}. It should be noted that all intercalates (except **3**) also exhibit a weak broad band between 1100 and 1000 cm^{-1}, which reveal the formation of a small amount of phosphate species.

XPS Studies

A detailed XPS study of $NiPS_3$ and of the investigated intercalates was performed at the 2*p* core levels of nickel, sulfur, and phosphorus atoms and 1*s* core levels of sodium, oxygen, and carbon atoms. Only those results relative to Ni, P, and S will be mentioned here.

The Ni 2*p* XPS spectrum of $NiPS_3$ is shown in Fig. 2. In agreement with previously reported results (11, 15) the Ni 2*p* XPS spectra of investigated samples consist of spin-orbit doublets $2p_{3/2}$ and $2p_{1/2}$, each component of the doublet showing a satellite feature. The best fit of the experimental spectrum is shown in Fig. 2 and the parameter values derived are listed in Table 2. Comparison of $NiPS_3$ before and after sodium intercalation shows relatively small changes in the spectra: the main line slightly shifts towards lower binding energies (about 0.2 eV) and the line width stays nearly constant. Only the satellites show some variations: the intensity of S_1 rises, while the energy of S_2 shifts toward higher binding energies with broadening of the line width.

The spectrum of the pyridinium intercalate **2** also appears very close to the spectrum of $NiPS_3$. The satellites show even smaller modifications with respect to $NiPS_3$ than **1**. However, when **2** is treated with sodium sulfide, much larger modifications occur: the main line in the spectrum of **5** has shifted by about 1 eV toward lower binding energies, the intensity of S_2 strongly decreases, and S_3 disappears. A very similar behavior is observed upon lithium intercalation in $NiPS_3$ ($Li_{1.5}NiPS_3$) (11).

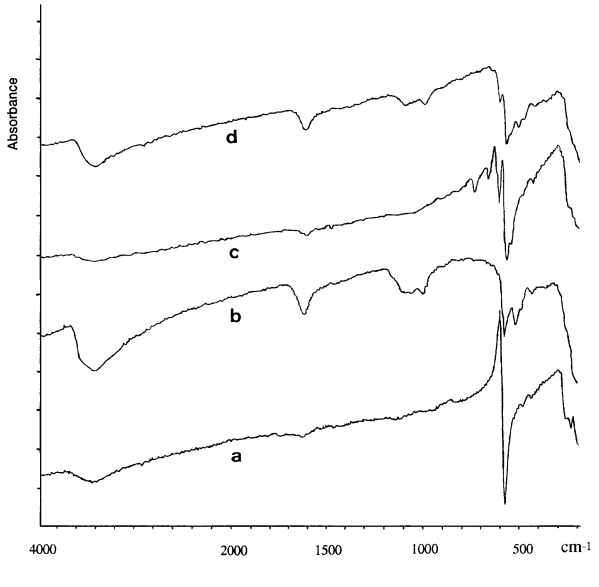

FIG. 1. Infrared spectra of (a) $NiPS_3$, (b) Na_xNiPS_3, (c) $NiPS_3(pyH)_y$, and (d) $Na_xNiPS_3(pyH)_\varepsilon$.

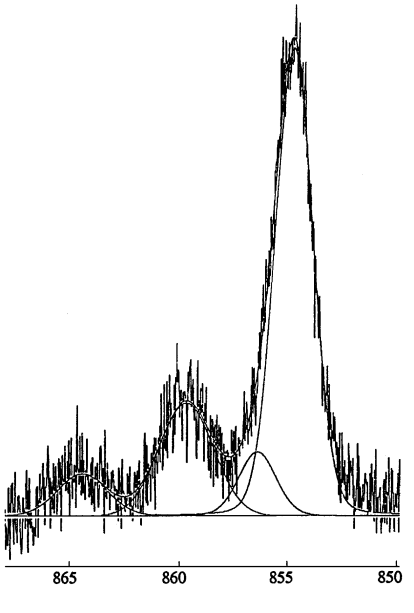

FIG. 2. X-ray photoemission spectrum of the Ni 2*p* core level for $NiPS_3$ showing best fit calculated lines of Ni $2p_{3/2}$ core level.

TABLE 2

Parameter Values Obtained from the Best Fit of Ni $2p_{3/2}$

Compound	E_b (eV) main peak	W (eV)	I	E_b (eV) S_1	D_1 (eV)	W_1 (eV)	I_1	E_b (eV) S_2	D_2 (eV)	W_2 (eV)	I_2	E_b (eV) S_3	D_3 (eV)	W_3 (eV)	I_3
$NiPS_3$	854.60	2.03	1	856.30	1.70	2.05	0.14	859.60	5.0	2.97	0.35	864.30	9.7	2.67	0.12
Na_xNiPS_3 **1**	854.45	2.06	1	856.20	1.75	3.66	0.66	861.35	6.9	3.96	0.36	864.26	9.8	3.35	0.12
$NiPS_3(pyH)_y$ **2**	854.40	1.95	1	856.20	1.80	2.23	0.33	859.60	5.2	2.91	0.49	864.00	9.7	3.30	0.36
$Na_xNiPS_3(pyH)_\varepsilon$ **5**	853.50	1.78	1	855.30	1.80	2.05	0.20	860.10	6.6	2.69	0.09				

Note. E is the position in binding energy; W is the full width at half maximum; I is the intensity calculated as the total area under each line, relative to the principal line; D is the separation of the satellite structure from the main line.

The 2*p* P and S XPS spectra of the same samples have been also performed. By deconvolution of the experimental peaks, the phosphorus spin-orbit $2p_{1/2}$–$2p_{3/2}$ components could be resolved. The positions in binding energy and the other characteristics of these peaks are reported in Tables 3 and 4. Computer simulation shows the existence of two types of phosphorus atoms: a first one around 132 eV is related to P in $NiPS_3$ (11, 15) and a second (around 134 eV) which is attributed to phosphorus atoms in an oxygenated environment. The binding energy of the former peak is slightly shifted in the intercalates with respect to $NiPS_3$, but the sign of the shift changes: from 0.6 toward higher energy for the sodium intercalate to 0.3 eV toward lower energy in the pyridinium case.

Only one type of sulfur atoms is evidenced from the XPS spectra. The binding energy in the sodium intercalate **1** is about the same as in pure $NiPS_3$, owing to the incertitude, but there is a significant decrease for the pyridinium intercalate. The most striking fact is the decrease by 0.7 eV in compound **5** (with respect to $NiPS_3$).

Catalytic Properties

Figure 3 displays typical kinetic curves of S^{2-} catalytic oxidation by O_2 to elemental sulfur in the presence of $NiPS_3$ and of different intercalates at room temperature and a 15 g/liter concentration of the sulfide ions. These results show that all intercalates exert a higher activity than pure $NiPS_3$.

A comparative study of the catalytic properties of these compounds at different temperatures ($T = 20, 30, 40, 50°C$) and different concentrations of the sulfide ions in aqueous solution ($C = 3$, 5, 10, 15, and 20 g S^{2-}/liter) confirms in all cases the higher activity of the intercalates. A parameter related to the activation energy can be calculated, assuming an Arrhenius temperature dependence of the reaction rate (for the same sulfide concentration at various temperatures). This parameter is found two times smaller on going from $NiPS_3$ to intercalates **2**, **3**, and **4** (48.3 kJ/mol for $NiPS_3$, 35.6 kJ/mol for the sodium intercalate **1**, 23.1 kJ/mol for the pyridinium intercalate **2**, and 22.8 kJ/mol for the polymer intercalate **4**). This tends to show that the higher activity of the intercalates cannot be due to smaller particle size only. In addition, the induction period observed in the case of $NiPS_3$ seems no longer to exist in the case of the intercalates, a feature which suggests that intercalation into pure $NiPS_3$ is a first prerequisite for catalysis to occur.

In runs, performed in the presence of a small amount of sulfide ions, a pause in the oxygen absorption was observed (Fig. 4). Oxygen absorption occurred again after readmission of sulfide ions into the solution and ceased again after consuming an amount of oxygen equal to the S^{2-} amount in the starting solution.

TABLE 3

Parameter Values Obtained from the Best Fit of the XPS Spectrum of the P 2*p* Core Level for $NiPS_3$, Na_xNiPS_3, $NiPS_3(pyH)_y$, and $Na_xNiPS_3(pyH)_\varepsilon$

Compound	$E_{2p_{3/2}}$ (eV)	W (eV)	I	$E_{2p_{1/2}}$ (eV)	W (eV)	I
$NiPS_3$	132.10	1.61	1	132.9	1.80	0.53
	134.50	1.62	0.19	135.3	1.79	0.10
Na_xNiPS_3 **1**	132.70	1.60	1	133.5	1.64	0.57
	134.50	1.60	0.28	135.3	1.73	0.14
$NiPS_3(pyH)_y$ **2**	131.80	1.42	1	132.6	1.55	0.56
	133.50	1.50	0.17	134.3	1.55	0.09
$Na_xNiPS_3(pyH)_\varepsilon$ **5**	131.95	1.63	1	132.7	1.65	0.57
	133.60	1.64	0.34	134.4	1.65	0.19

TABLE 4

Parameter Values Obtained from the Best Fit of the XPS Spectrum of the S 2*p* Core Level for $NiPS_3$, Na_xNiPS_3, $NiPS_3(pyH)_y$, and $Na_xNiPS_3(pyH)_\varepsilon$

Compound	$E_{2p_{3/2}}$ (eV)	W (eV)	I	$E_{2p_{1/2}}$ (eV)	W (eV)	I
$NiPS_3$	162.4	1.41	1	163.6	1.42	0.56
Na_xNiPS_3 **1**	162.5	1.60	1	163.7	1.68	0.57
$NiPS_3(pyH)_y$ **2**	162.1	1.60	1	163.3	1.60	0.59
$Na_xNiPS_3(pyH)_\varepsilon$ **3**	161.7	1.32	1	162.7	1.38	0.57

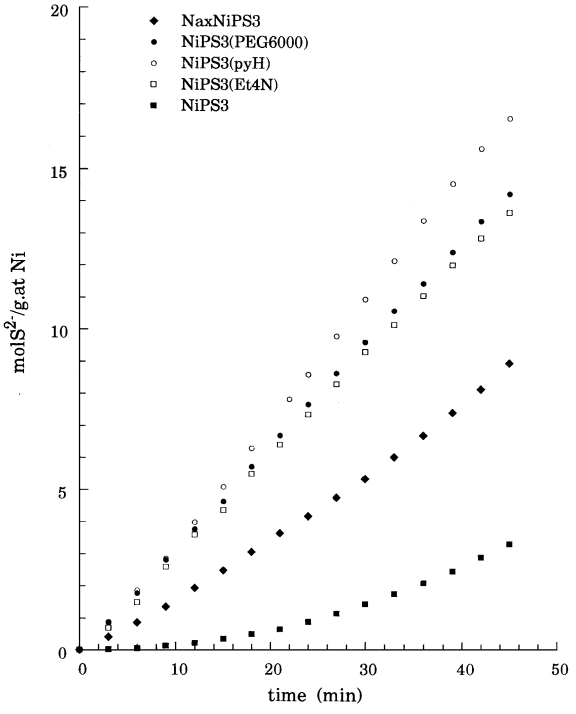

FIG. 3. Kinetic curves of the sulfide ion catalytic oxidation. Sulfide ions concentration 15 g/liter ($T = 20°C$).

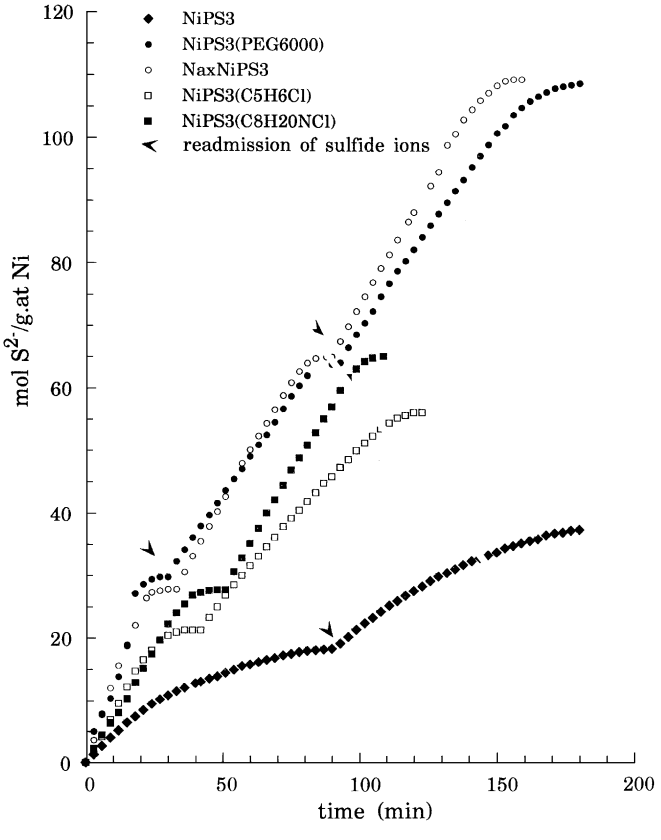

FIG. 4. Kinetic curves of the sulfide ion catalytic oxidation. Sulfide ions concentration 3 g/liter ($T = 20°C$).

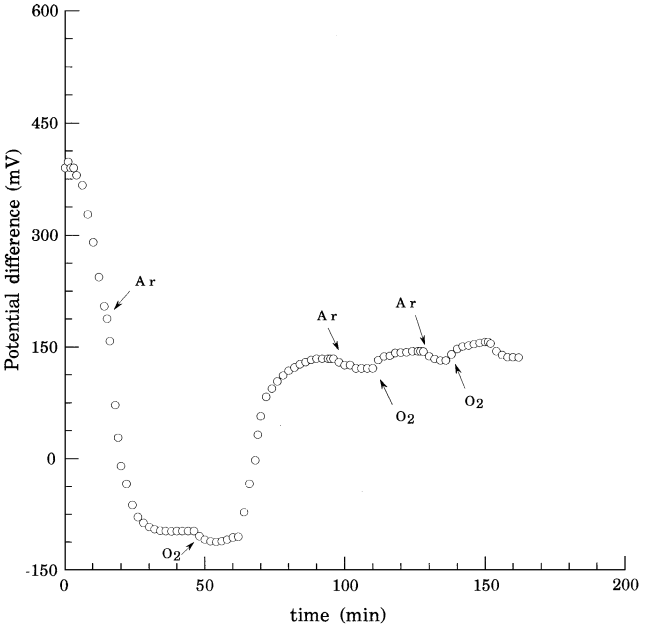

FIG. 5. Variation of the potential difference between the catalyst-containing electrode and the calomel electrode, dipped in a Na_2S aqueous solution, during consecutive purging with Ar and O_2.

The electrochemical measurements show an evolution of the potential difference between the electrode containing the investigated sample (pure or intercalated $NiPS_3$) and the calomel electrode on successive purging with argon and oxygen. In argon flow, the potential difference was systematicaly shifted to negative values, whereas oxygen displaced the potential difference to positive values. This is illustrated in Fig. 5 for the pyridinium intercalate. These results clearly indicate that the sulfide ions present in the solution lower the potential of the host lattice, while oxygen increases it.

DISCUSSION

The suggested mechanism of the catalytic act has been postulated (2) to involve intercalation and deintercalation processes as principal steps, accompanied by redox modification of the host lattice, according to the schemes

$$x\mathrm{Na}^+ + x/2\mathrm{S}^{2-} + y(\mathrm{H_2O}) + [\mathrm{NiPS_3}] \rightarrow (\mathrm{Na}^+)_x(\mathrm{H_2O})_y[\mathrm{NiPS_3}]^{x-} + x/2\mathrm{S}^0 \quad [2]$$

$$(\mathrm{Na}^+)_x(\mathrm{H_2O})_y[\mathrm{NiPS_3}]^{x-} + x/2\mathrm{O_2} \rightarrow x\mathrm{Na}^+ + (y-x)\mathrm{H_2O} + [\mathrm{NiPS_3}] + 2x\mathrm{OH}^-. \quad [3]$$

Our results unambiguously show that the intercalates of $NiPS_3$ have a greater efficiency to catalyze oxydation of sulfide ions than pristine $NiPS_3$. If the postulated mechanism is true, this higher efficiency should be correlated to a greater ability of the lattice to accomodate the electrons released by the sulfide ions. The electronic structure of the various

intercalates should therefore be a crucial point, and hence the first question which arises is that of the modification of the electronic structure of $NiPS_3$ upon intercalation.

As discussed below, it turns out that intercalation of sodium ions into $NiPS_3$ from a Na_2S solution is less simple than lithium insertion from butyllithium. The analytical data of (**1**) indicate, as noted already in Ref. (12), that significant chemical changes of the host material accompany the first (sodium) intercalation step. In particular, there seems to be a significant loss of about 10% of phosphorus. Infrared spectroscopy in the region below 600 cm^{-1} confirms that a fraction of the PS bonds are modified. The appearance of a band at 520 cm^{-1} in the IR spectrum of the sodium intercalate (**1**) may actually be the signature of the stretching band of thiophosphate (V) PS_4^{3-} groups (16). This would mean that whereas most of the P_2S_6 groups of the host structure are retained (persistance of the 570 cm^{-1} band), a fraction would decompose into PS_4^{3-} anions, this process leading to the release of some phosphorus. XPS and IR spectrocopy indicate the presence of phosphate species. Actually these phenomena may be only side effects and they do not prove that the phosphorus deficit compensate for the guest cationic charge, but at least they indicate that should reduction of the $NiPS_3$ lattice actually occur, this is by no means the only feature going on.

The appearant deficit of phosphorus in (**1**) could also be regarded as an excess of sulfur atoms that could result from the cointercalation of both Na^+ and S^{2-} ions. Following the remarks of one referee, the weak band around 520 cm^{-1} might be alternatively assigned to polysulfide species which would result from the reaction between the entering sulfide ions with the P_2S_6 units. Although this possibility cannot be ruled out on the basis of the present results, it seems quite unlikely on the basis of the following arguments: (i) spectrocopic studies (17–19) have shown that the S–S vibrations in several polysulfides occur at significantly lower wevenumbers, below 490 cm^{-1}; (ii) The formation of polysulfide intercalates in MPS_3 or MS_2 layered compounds has never been reported.

XPS is a technique in which one probes the electron environment of different atoms or ions, but because relaxations or secondary excitations are always associated with core-hole production, it is generally difficult to determine the precise correspondance between XPS peaks and ground state properties. For transition-metal compounds the chemical shifts involving the main line are generally small, even when large cation valence changes are involved (20). Greater chemical sensitivity is found at the satellites. The chemical changes can be monitored by measuring the relative separations between the main line and the satellites. By comparison with other Ni compounds (21, 22), S_2 and S_3 satellites in the spectrum of $NiPS_3$ can be interpreted as ligand-to-metal charge transfer shake-up transitions, while S_1 may be attributed to a multiplet splitting effect.

The nickel XPS spectrum of the sodium intercalate **1** shows only little changes with respect to $NiPS_3$, both in the main line position and in satellite intensity. The main line is shifted only by 0.15 eV toward lower energy, which indicates a weak level of reduction of the nickel ions. This contrasts with the much larger shift observed for a lithium intercalated $NiPS_3$ (Li_xNiPS_3) even when $x < 0.37$ which has been interpreted as the result of electron transfer from the 2*s* lithium electrons into the Ni 4*s* states (11). The observed shift of S_2 toward higher binding energies can be related to a greater positive charge at the cation site, which may be related to the change in the binding energy of phosphorus. The latter may be tentatively explained by the presence of PS_4^{3-} ions in which the phosphorus atoms are in the +5 oxidation state. The formation of such species is consistent with the loss of phosphorus evidenced by the analytical data. However the phosphoruos XPS spectra give evidence for only one type of phosphorus bonded to sulfur atom, whereas infrared spectroscopy shows that P_2S_6 groups are still present in the host lattice. We have no clear explanation for this appearant discrepancy. One possibility is that a larger amount of the PS_4^{3-} ions are formed near the surface of the crystals, which is the region probed by the XPS method. In any case, the following conclusion can be drawn: (i) the chemistry leading to the formation of the $NiPS_3$ sodium intercalate **1** is more complex than the chemistry of lithium insertion into $NiPS_3$ from butyllithium reagent (9); (ii) there is little reduction of the nickel ions if any, at least near the surface of the $NiPS_3$ crystals, which is also the region of interest for heterogeneous catalysis. It is worth recalling also from Ref. (12) that the XANES study at the Ni *K*-edge of the sodium intercalate does not show any shift indicating reduction. Therefore, charge compensation for the entering sodium cations in **1** might well occur, at least in part, through the loss of part of the phosphorus (IV) atoms of the P_2S_6 groups or alternatively, as discussed above, by the insertion of sulfide ions.

The treatment of the sodium intercalate **1** by pyridinium chloride has a noticeable effect on both the IR spectra and the XPS spectrum. The 520 cm^{-1} IR band of the sodium intercalate has disappeared in the spectrum of **2**, and a sharp band appears at 610 cm^{-1}. It therefore appears that the postulated PS_4^{3-} species have been transformed. This is not surprising, as such species are known to be easily hydrolyzed; they may be quite stable as long as the medium is basic, but pyridinium ions have an acidic character which cause decomposition. This view is consistent with the disappearance in the phosphorus XPS spectrum of **2** of the 132.7 eV line attributed to the PS_4^{3-} species present in **1**. The phosphorus main line is found at 131.8 eV in **2**, at slightly lower energy than in pristine $NiPS_3$. Therefore, the XPS main lines of Ni, P, and S in the pyridinium intercalate **2** are all very slightly shifted toward lower energy with respect to pristine $NiPS_3$, which is consistent

with a small extent of reduction of the host lattice due to intercalation.

When the pyridinium intercalate **2** is further treated by sodium sulfide (to simulate catalysis conditions), the XPS lines of nickel in **5** are found at much lower binding energy, as well as the line of the sulfur atoms, which are bonded to the nickel. This definitely shows that the nickel ions in the pyridinium intercalate **2** are now strongly reduced, to a level comparable to that in the Li_xNiPS_3 ($x > 1$) intercalates, where a formation of Ni^0 domains has been suggested (9).

We have therefore reached a point where it appears that the sodium intercalate **5** obtained after a three-step treatment is much more deeply reduced than the sodium intercalate **1** obtained directly from pure $NiPS_3$. Although we have no definite explanation for this surprising fact, we can nevertheless suggest that the lower extent of reduction on going from pristine $NiPS_3$ to **1** is related to the chemical modifications undergone by the host lattice.

Most important, there appears to be an obvious correlation between the aptitude of the various materials to be efficiently reduced and their ability to catalyze the oxidation process of sulfide ions. The activation energy is about two times lower for the pyridinium intercalate (and the PEO intercalate as well) than for pure $NiPS_3$. Therefore, our results support the mechanism proposed in Ref. (2). The fundamental point is that the $S^{2-} \rightarrow S^0 + 2e^-$ oxidation process is assisted by the host lattice which captures the electrons (together with sodium cations) to give an intercalate. It is then logical that the more deeply the lattice can be reduced, the more efficient it should be for catalysis.

Additional factors may also be responsible for the higher efficiency of the intercalates. In the case of pristine $NiPS_3$, sodium ions do not penetrate the catalyst galleries so easily (an induction period is observed) and the "working" nickel ions are those at the edge sites. In intercalates, a larger amount of sodium ions enters the larger interlayer space and nickel ions from the "inside surface" may take part in the catalytic cycle, thus giving rise to higher catalytic activity. Moreover, as already discussed in Ref. (2), the inserted water molecules which solvate the guest cations are likely to be activated by polarization effects. Finally, the higher activity of intercalates could also arise from their more dispersed state, although the decrease of the pseudoactivation energy cannot be accounted for by this factor only.

In order to confirm sequences of oxidation and reduction cycles over the catalytic process (associated to intercalation–deintercalation processes), a series of electrochemical measurements were conducted under conditions which simulate Eqs. [2] and [3]. Under an inert atmosphere, conditions for reaction [2] are created, while in presence of oxygen the reaction [3] is favored. On purging with argon the potential difference between the two electrodes is shifted to negative values, while the opposite effect is observed in oxygen flow. These reversible and reproducible processes therefore support the idea that on dipping $NiPS_3$ and its intercalates into Na_2S solution, oxidation–reduction cycles of the suggested catalytically active sites (nickel ions) take place.

CONCLUSION

The present work therefore confirms the previouly suggested intercalation mechanism of catalytic performance in the reaction of sulfide ion oxidation over $NiPS_3$. It also provides a deeper insight into the phenomena that accompany $NiPS_3$ intercalation and allows a reasonable understanding of the higher activity of the $NiPS_3$ intercalates with respect to pristine $NiPS_3$. Attempts are in progress to examine the effect of substitution of part of the nickel ions by Cu(I) and Fe(II) ions on the catalytic activity and also to prepare these catalysts in a more dispersed state to design novel more effective catalysts for the sulfide oxidation reaction.

REFERENCES

1. Chen, K. Y., and Morris, J. C., *Environ. Sci. Technol.* **6**, 529 (1972).
2. Andreev, A., Ivanova, V., Kirilov, K., and Passage, G., *Appl. Catal. A: Gen.* **107**, 189 (1994).
3. Brec, R., *Solid State Ionics* **22**, 3 (1986).
4. O'Hare, D., *in* "Inorganic Materials" (D. Bruce and D. O'Hare, Eds.), p. 171. Wiley, New York, 1996.
5. Clement, R., Garnier, O., and Jegoudez, J., *Inorg. Chem.* **25**, 1404 (1986).
6. Brec, R., Schleich, D., Ouvrard, G., Louisy, A., and Rouxel, L. J., *Inorg. Chem.* **18**, 1814 (1979).
7. Colombet, P., Ouvrard, G., Antson, O., and Brec, R., *J. Magn. Magn. Mater.* **71**, 100 (1987).
8. Berthier, C., Chabre, Y., and Minier, M., *Solid State Commun.* **28**, 327 (1978).
9. Ouvrard, G., *in* "Chemical Physics of Intercalation II" (P. Bernier *et al.*, Eds.), Vol. 305, p. 315. Plenum, New York, 1993.
10. Giunta, G., Grasso, V., Neri, F., and Silipigni, L., *Phys. Rev. B* **50**, 49 (1994).
11. Curro, G. M., Grasso, V., Neri, F., and Silipigni, L., *Il Nuovo Cimento* **17D**, 37 (1995).
12. Doeuff, M., Cartier, C., and Clement, R., *J. Chem. Soc. Chem. Commun.*, 629 (1988).
13. Klingen, W., Oh, R., and Hahn, H., *Z. Anorg. Allg. Chem.* **401**, 97 (1973).
14. Lagadic, I., Léaustic, A., and Clement, R., *J. Chem. Soc. Chem. Commun.*, 1396 (1992).
15. Piacentini, M., Khumalo, F. S., Olson, C. G., Anderegg, J. W., and Lynch, D. W., *Chem. Phys.* **65**, 289 (1982).
16. Sala, O., and Temperini, M. L. A., *Chem. Phys. Lett.* **36**, 652 (1975).
17. Janz, G. J., Downey, J. R., Jr., Roduner, E., Wasilczyk, G. J., Coutts, J. W., and Eluard, A., *Inorg. Chem.* **15**, 1759 (1976).
18. Janz, G. J., Roduner, E., Coutts, J. W., and Downey, J. R., Jr., *Inorg. Chem.* **15**, 1751 (1976).
19. Janz, G. J., Coutts, J. W., Downey, J. R., Jr., and Roduner, E., *Inorg. Chem.* **15**, 1755 (1976).
20. Veal, B. W., and Paulikas, A. P., *Phys. Rev. B* **31**, 5399 (1985).
21. Zaonen, J., Westa, C., and Sawatzky, G. A., *Phys. Rev. B* **33**, 8060 (1986).
22. Okada, K., and Kotani, A., *J. Phys. Soc. Jpn.* **60**, 772 (1991).